RSC Advances

PAPER

View Article Online
View Journal | View Issue

Cite this: *RSC Adv.*, 2016, **6**, 66324

High performance CO_2 filtration and sequestration by using bromomethyl benzene linked microporous networks†

Ruh Ullah,‡[a] Mert Atilhan,*[a] Baraa Anaya,[a] Shaheen Al-Muhtaseb,[a] Santiago Aparicio,[b] Damien Thirion‡[c] and Cafer T. Yavuz*[cd]

Porous solid sorbents have been investigated for the last few decades to replace the costly amine solution and explore the most efficient and economical material for CO_2 capture and storage. Covalent organic polymers (COPs) have been recently introduced as promising materials to overcome several issues associated with the solid sorbents such as thermal stability and low gas capturing capacity. Herein we report the synthesis of four COPs and their CO_2, N_2 and CH_4 uptakes. All the presented COP materials were characterized by using an elemental analysis method, Fourier transform infrared spectroscopy (FTIR) and solid state nuclear magnetic resonance (NMR) spectroscopy techniques. The physical properties of the materials such as surface area, pore volume and pore size were determined by BET analysis at 77 K. All the materials were tested for CO_2, CH_4 and N_2 adsorption through a volumetric method using magnetic sorption apparatus (MSA). Among the presented materials, COP-118 has the highest surface area of 473 m^2 g^{-1} among the other four materials and has shown excellent performance by capturing 2.72 mmol g^{-1} of CO_2, 1.002 mmol g^{-1} of CH_4 and only 0.56 mmol g^{-1} of N_2 at 298 K and 10 bars. However the selectivity of another material, COP-117-A, was better than that of COP-118. Nevertheless, the overall performance of the latter has indicated that this material can be considered for further exploration as an efficient and cheaply available solid sorbent compound for CO_2 capture and separation.

Received 26th May 2016
Accepted 30th June 2016

DOI: 10.1039/c6ra13655a

www.rsc.org/advances

1. Introduction

The overwhelming scientific concerns about global warming caused by anthropogenic carbon dioxide (CO_2) emissions has driven the attention of scientists to explore techniques and materials that can effectively create alternative solutions to mitigate hazardous greenhouse emissions that are generated during the processing of fossil based hydrocarbon sources.[1] Techno-economic analysis[2] has revealed that using aqueous mono-ethanol amine (MEA) based solution scrubbing techniques employed both in pre- and post-combustion CO_2 capture processes[3,4] has major drawbacks such as amine degradation, thermal instability, high corrosivity and an intense energy need during the solvent regeneration step. Therefore, the need for searching for more effective, cleaner, safer, environmentally friendlier and cheaper materials and technologies are underway[5] in order to overcome aforementioned issues for commercialized CO_2 capturing systems in power plants and other chemical process industries for flue gases emission mitigation and control.[6] Surely, the flue gases capture and storage systems including carbon capture and storage (CCS) requires materials with high capturing capacity, tunable selectivity amongst the various targeted gases, robust physical and chemical structure that can withstand severe process pressure and temperature conditions, and they can be used repeatedly for numerous cycles without any significant loss of in efficiency.[7] As an alternative approach, solid materials have been emerged as the best option as long as the robustness, reproduction and reusability of the absorbent materials are concern.[8] Glier *et al.*[9] has compared the CO_2 capturing efficiency of solid materials with the commonly used amine solution and suggested that metal–organic framework (MOF) based sorbents are about 4–5% more efficient and require less energy to be reproduced and they can be used repeatedly. On the other hand, despite their fascinating chemical structures, it has been reported poor gas selectivity (*e.g.* CO_2/CH_4) at typical process operating conditions with MOFs.[10] Gas selectivity[11] for flue gases can be tuned up by using different linker materials within covalent organic frameworks (or covalent organic polymers – COPs) and this would not only improve the gas selectivity but also lead to substantial improvements in the

[a]*Department of Chemical Engineering, Qatar University, Doha, Qatar. E-mail: mert.atilhan@qu.edu.qa*

[b]*Department of Chemistry, University of Burgos, 09001 Burgos, Spain*

[c]*Graduate School of EEWS, KAIST, Daejeon 305-701, Republic of Korea*

[d]*Department of Chemistry, KAIST, Daejeon 305-701, Republic of Korea. E-mail: yavuz@kaist.ac.kr*

† Electronic supplementary information (ESI) available. See DOI: 10.1039/c6ra13655a

‡ Equal contribution.

CO_2 capture capacity.[12–15] This has been demonstrated in several works. Lu *et al.*[16] prepared highly porous polymer networks (PPN) and modified CO_2 adsorption capacities by grafting sulfonic acid (SO_3H) and lithium sulfonate (SO_3Li), which also improved the selectivity of CO_2 over N_2 and was reported as 155 and 414 for PPN-6-SO_3H and PPN-6-SO_3Li respectively at room temperature and 1 bar.[16] Recent studies have shown that covalently bonded and purely organic polymers which have high hydrothermal stability, highly porous structures and have very large heat of adsorption can adsorb significant amount of CO_2.[17] It was further noted that for post-combustion process at lower pressures, increase in isosteric heat of adsorption incorporated by the introduction of base functionalities in micro-porous polymer network, is the origin of CO_2 uptake and lower energy requirement for the material regeneration rather than the pore volume.[18,19] However, for high pressure CO_2 uptake, both base functionality and pore volume contribute to the adsorption process of porous polymer network.[18] Patel *et al.* has shown that amorphous porous polymer modified with azo group (–N=N–) possess very high thermal stability, have large surface area, can store enormous amount of CO_2 with excellent selectivity against N_2 and can maintain the capturing capacity even after boiling in water for a long time.[20] CO_2 uptake of covalent organic polymer at room temperature and 1 bar was further increased up to the maximum of 5.19 mmol g^{-1}, by introducing tetra-anilyladamantane (TB) as tertiary amino linkers.[21] Comparing the production cost and CO_2 capturing capacity at high pressure up to 200 bars of COP-1 to that of MEA solution, Patel *et al.*[12] has suggested that covalent organic polymer could store significantly large quantity of CO_2 at low economic cost. However, by inserting sulfur into the covalent organic polymer structure, the CO_2 uptake has gone down from 5616 mg g^{-1} (COP-1)[12] to 3294 mg g^{-1} (ref. 13) at 318 K and 200 bar.[13] Z. Xiang *et al.*[17] has tested several covalent organic polymers (COPs) for adsorption of other gases such as O_2, N_2, H_2 and CH_4 and pointed out that COP-4 can adsorbed 594 mg g^{-1} of CO_2 at 298 K and 18 bars.

Although, most of the literature so far is mainly devoted to the adsorption and selectivity of CO_2, there is limited experimental study on the capturing capacity of COPs for other constituents of flue gases including CO_2, CH_4 and N_2 at near process partial pressure conditions for these gases. Based on the tunable properties *i.e.* BET surface area, pore volume, capturing capacity and possible low cost regeneration and recyclability, three different structures of covalent organic polymers have been prepared in this work and we report the synthesis, characterization and gas sorption testing of 3 different COPs. The main focus of this work is to investigate CO_2 adsorption and desorption performance of the presented COPs and check their suitability at wide pressure and temperature CO_2 capture applications. Moreover, in order to complement the work, sorption performance of additional gases, N_2 and CH_4, at wide pressures and temperatures have also been carried out to calculate the gas selectivity performance of the presented materials.

2. Experimental

2.1 Materials and methods

All reagents were purchased from Sigma-Aldrich and TCI, which were used without further purification. Solvents were purchased from Samchun Pure Chemicals (S. Korea), dichloroethane was distilled over P_2O_5 under argon prior to use.

Elemental analysis was performed at the KAIST Central Research Instrument Facility on Thermo Scientific FLASH 2000 equipped with a TCD detector. Solid-state ^{13}C and ^{31}P cross-polarization magic angle spinning NMR (CP-MAS) were performed at the KAIST Central Research Instrument Facility on a Bruker Advance 400 MHz WB equipped with a 4 mm probe. The contact time was 5 ms with a delay of 3 s, where, samples were spun at 12 kHz for ^{13}C and 20 kHz for ^{31}P experiments. Fourier transform infrared spectra (FTIR) were recorded on a Shimadzu IR-Tracer-100 equipped with a Gladi ATR module. Textural characterization of polymers was carried out from nitrogen adsorption isotherms using a Micrometrics 3FLEX accelerated surface area and porosimetry analyzer at 77 K. The specific surface areas were derived from Brunauer–Emmett–Teller (BET) method. Average pore diameter data were also determined by using the BJH desorption model. Prior to sorption measurement, samples were activated through a degassing step at 423 K for 5 hours under vacuum, which was applied by a mechanical roughing pump, manufactured by Varian Inc. All the COP materials that are reported herein were synthesized in a similar procedure and they are described below.

2.2 Procedure for COP-117-A

Mesitylene (0.83 mL, 0.72 g, 6 mmol) and α,α′-bis-bromoxylene (2.38 g, 9 mmol) were dissolved in 60 mL dry dichloroethane under argon. Aluminum(III) chloride (2.40 g, 18 mmol) was added portion wise and the solution was heated up to 80 °C under vigorous stirring with the presence of argon for 24 h. The reaction was then allowed to cool to room temperature and after that water was added and the obtained solid was filtered, washed extensively with water and methanol until the filtrate became clear. Then the solid is redispersed in MeOH/HCl, sonicated for 20 minutes, filtered and washed again with MeOH and THF. After drying for 12 h under vacuum at 80 °C, COP-117-A was obtained as a brown powder (2.01 g). Elemental analysis found (theoretical): % C 81.11 (91.75), % H 6.56 (8.25); FTIR (ATR, cm^{-1}): 2962, 2920, 2868, 1690, 1617, 1450, 1377, 1058, 880; ^{13}C CP-MAS NMR (δ_C, ppm): 155 (C and CH aromatic), 58 (CH_2), 40 (CH_3).

2.3 Procedure for COP-117-B

According to the general procedure but by replacing aluminum(III) chloride by zirconium(IV) chloride (4.08 g, 18 mmol). After drying for 12 h under vacuum at 80 °C, COP-117-B was obtained as a brown powder (1.40 g). Elemental analysis found (theoretical): % C 87.93 (91.75), % H 6.72 (8.25); FTIR (ATR, cm^{-1}): 2996, 2913, 2861, 1607, 1503, 1440, 1180, 1013, 888, 804, 752; ^{13}C CP-MAS NMR (δ_C, ppm): 161 (C and CH aromatic.), 153 (C and CH aromatic.), 61 (CH_2), 44 (CH_3).

2.4 Procedure for COP-118

Same procedure as for COP-117-A but by replacing mesitylene with triphenylphosphine (1.57 g, 6 mmol) and aluminum(III) chloride with iron(III) chloride (2.92 g, 18 mmol). After drying for

12 h under vacuum at 80 °C, COP-118 was obtained as a brown powder (1.12 g). Elemental analysis found (theoretical): % C 72.71 (84.12), % H 4.59 (7.20); FTIR (ATR, cm^{-1}): 3002, 2918, 1678, 1605, 1511, 1438, 1261, 1188, 1115, 885, 812, 750, 719, 687, 541; ^{13}C CP-MAS NMR (δ_C, ppm): 156 (C and CH aromatic), 58 (CH_2), 40 (CH_3); solid state ^{31}P NMR (δ_P, ppm): −41.49.

2.5 Procedure for COP-119

Same procedure as for COP-117-A but by replacing α,α′-bis-bromoxylene with trisbromomethylbenzene (2.14 g, 6 mmol). After drying for 12 h under vacuum at 80 °C, COP-119 was obtained as a brown powder (1.49 g). Elemental analysis found (theoretical): % C 85.57 (91.75), % H 6.91 (8.25); FTIR (ATR, cm^{-1}): 2960, 2926, 2874, 1687, 1614, 1447, 1375, 1072, 1020, 875, 765; ^{13}C CP-MAS NMR (δ_C, ppm): 162 (C and CH aromatic), 155 (C and CH aromatic), 61 (CH_2).

2.6 Gas adsorption measurements

Magnetic sorption apparatus (MSA) from Rubotherm Prazisionsmesstechnik® was used to measure CO_2 adsorption at high pressure up to 10 bars and different isotherms. Temperature of the sample was maintained through external temperature constant temperature thermo-stating bath (from Polyscience Inc.). Details of the experimental set up for high pressure gas measurement are available in detail elsewhere.[22] Gas sorption measurements start with activation of the material and in a typical procedure a known amount of material is degassed with Micromeritics ASAP 2420 for 5 hours at 200 °C and was then kept in MSA sample holder for further evacuation at 110 °C for 5 hours. After evacuation, mass and volume of the sample was determined by adsorption–desorption of helium gas. The maximum set pressure (10 bars) was applied stepwise by increasing the pressure gradually from 1 bar up to 10 bars. Each pressure point took about 60 minutes to gain the stable pressure set point and temperature equilibrium. During this period, four different sets of measurements were recorded and lowest standard deviation set of data was collected and used for further data analysis. MSA system is fully automated and the pressure goes to next higher point after completing the previous measurement point. The system was also depressurized gradually from 10 bars to evacuation stage in order to obtain desorption behavior and hysteresis effect on the experimented materials. The details of the apparatus description, operating principle and its schematic drawings are given in the ESI† document of this work. Density of the adsorbed He was calculated with the help of following eqn (1).

$$\rho_{He} = \frac{PM}{RT} \quad (1)$$

where ρ_{He} is the density of adsorbed helium gas, P is the given pressure, which varies from 1 bar to 10 bars, M is the molecular weight of helium, R is the real gas constant and T is the absolute temperature. The graph (ESI Fig. S2†) between adsorbed quantities of He *versus* density of the adsorbed gas gives a linear behaviour with the following eqn (2).

$$y = mx + c \quad (2)$$

In eqn (2), slope (m) of the straight line represents the combined volume of the used sample and the sample holder while the y-intercept (c) is the mass of adsorbent material. After determination of the mass and volume of the adsorbent materials with the above procedure, density of the sample is calculated and then the same sample was ready to be used for further sorption experiments with other gases, CO_2, CH_4 and N_2, at 298 K and 323 K isotherms respectively. After each run for different gases sample was evacuated for at least 6 hours at 110 °C to confirm the complete bareness of the sample from the previously used gas and possible moisture that is carried from the gas cylinder. Density of the adsorbed gases (CO_2, CH_4, and N_2) was determined with the similar procedure used for He measurement, however, compressibility factor of the corresponding gases were also included in the calculation. Further checks for the *in situ* gas density experimental data was obtained by using NIST REFPROP 9.0 software,[23] which is a current reference database software for obtaining the pure gas densities including CO_2, CH_4, and N_2. The amount of adsorbed gas per gram of the adsorbent was calculated for each pressure valve at a constant temperature after calculating the density of the gas from the corrected weight data obtained with MSA. Detailed data table can be found in the ESI.†

Moreover, the interaction of CO_2 and COP material was studied by using *in situ* FTIR technique with the use of high temperature reaction chamber (HVC) in conjunction with Praying Mantis™ accessory, supplied by Harrick™ Scientific, which were placed in Bruker® Vertex 80 FTIR Spectrometer. In order to guarantee sufficient infrared beam penetration in the sample, the subjected sample to diffuse reflectance is typically diluted with a material that is transparent in the infrared region, and this dilution should be based on 1 to 5 weight per cent. Hence, COP-118 was prepared by diluting it with spectroscopic grade KBr powder, provided by Harrick™ Scientific, with a sample to KBr ratio of 3 wt%. Spectral subtraction was performed to eliminate the contribution of CO_2 in the bulk of HVC. A spectrum of pure KBr powder exposed to CO_2 is subtracted from a spectrum of the diluted COP material exposed to CO_2 at exactly same pressure under 298 K. To ensure the lack of OH stretch band contribution, moisture content in the diluted COP material and pure KBr was taken out by subjecting them to evacuation, and later by vacuuming the system for at least 1 hour after placing each material in HVC. Temperature stability was obtained *via* maintaining a thermo-regulator to operate at 298 K isotherm overnight. Spectra of COP material exposed to different pressures of CO_2 were carefully collected after allowing at least 5 minutes for adsorption to take place. Beyond the reported pressure values, the spectra become dominated by gaseous CO_2 in the bulk, hindering the identification of bands that correspond to CO_2 interacting with COP material.

3. Results

In order to design a porous polymer with high gas uptake performance at high pressures, we first looked into the

chemistry of the monomers. For CO_2 capture, heteroatoms that can interact with the quadruple of the molecule would be ideal as well as the micropores. Methane, on the other hand required purely hydrocarbon network and alkyl substituents are expected to contribute to the adsorption. Nitrogen adsorption is not wanted since most gas separations require N_2 to not be associated with the sorbent. It is, however, hard to prevent, since the micropores and high surface area will serve as adequate means for its systematic uptake. In this work, we designed and synthesized three covalent organic polymers, COPs 117, 118 and 119 (Fig. 1). Bidentate and tridentate linkers based on bromomethyl benzenes are used to crosslink mesitylene and triphenyl phosphine. In the case for mesitylene, directing the crosslinking to specific sites in between the methyl substituents is expected, although at the expense for reactivity in the case of bidentate linker.

3.1 Synthesis and characterization

The porous polymer networks were all synthesized through Friedel–Crafts alkylation of a bis- or tris-brominated linker and an aromatic core promoted by a metallic Lewis acid (Fig. 1). In order to understand their structures, the resulting networks were studied by solid state NMR, FTIR and elemental analysis.

One important side reaction of the Friedel–Crafts alkylation that needs to be checked is the self-condensation of the halogenated linkers.[24,25] To confirm that the desired COP networks have been formed, the presence of the core in the network has been studied through ^{13}C solid state NMR (Fig. 2). The ^{13}C solid-state NMR of the COP networks is similar with two distinct regions of peaks. COP-117-A, B and COP-119 show two peaks at 40 and 60 ppm that can be attributed to the methyl from the core and methylene bridges from the linker respectively. The peaks of COP-117-B are better defined than those of COP-117-A and COP-119. COP-117-B was synthesized by using zirconium chloride instead of aluminum chloride, which possibly gave a cleaner structure of with less crosslinking because of the different reactivity.[26] COP-118 possessing a different core shows only the peak at 61 ppm corresponding only to the methylene bridges. The presence of the triphenylphosphine core in the structure is confirmed through ^{31}P solid state NMR with a single peak at −41 ppm (ESI†). The second region of peaks in the spectra is between 145 and 170 ppm and can be attributed to the aromatic C and CH in the structures. In COP-117-B and COP-118 it is possible to differentiate two distinct maxima at 155 and 161 ppm whereas in COP-117-A and COP-119 there is only one broad peak around 156 to 160 ppm. The ^{13}C and ^{31}P solid-state NMR study confirms the presence of the different cores in the COP structures and not networks of self-condensated linkers. Of course, one might expect a degree of deviation, however, our repetitive syntheses and analyses gave similar results.

Elemental analysis was performed on all COPs and the results are given at Table 1. Experimental and theoretical values differ by up to 11% in carbon content and 2.7% in hydrogen content in these structures. These differences are not

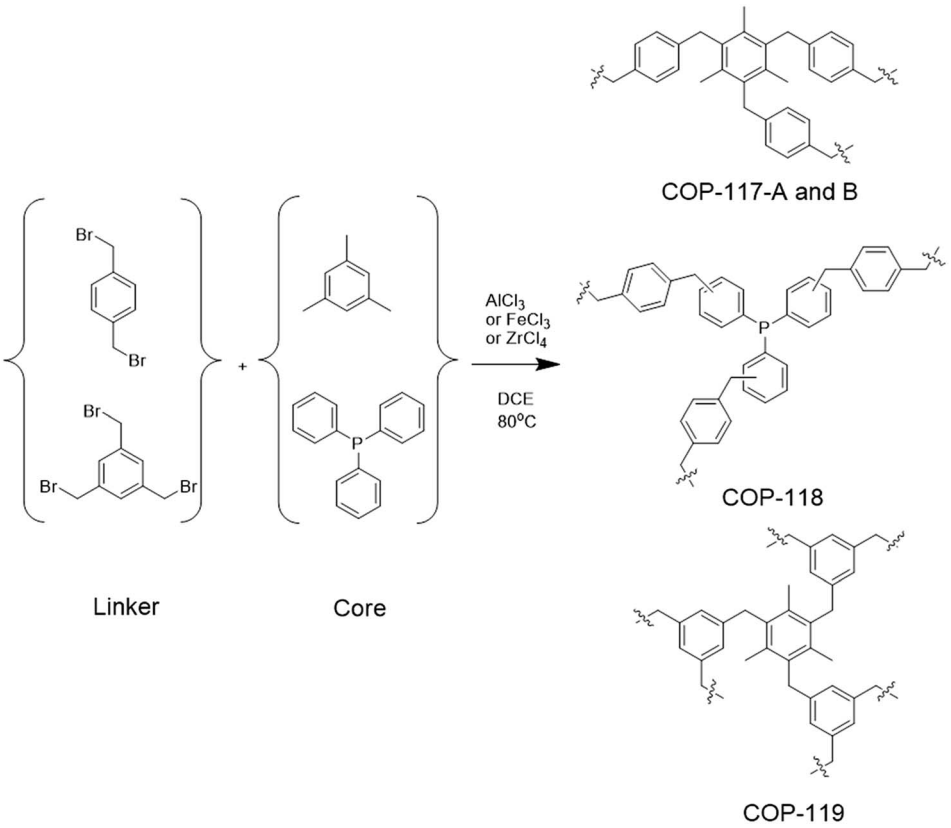

Fig. 1 Synthesis and expected structures of COPs presented in this manuscript.

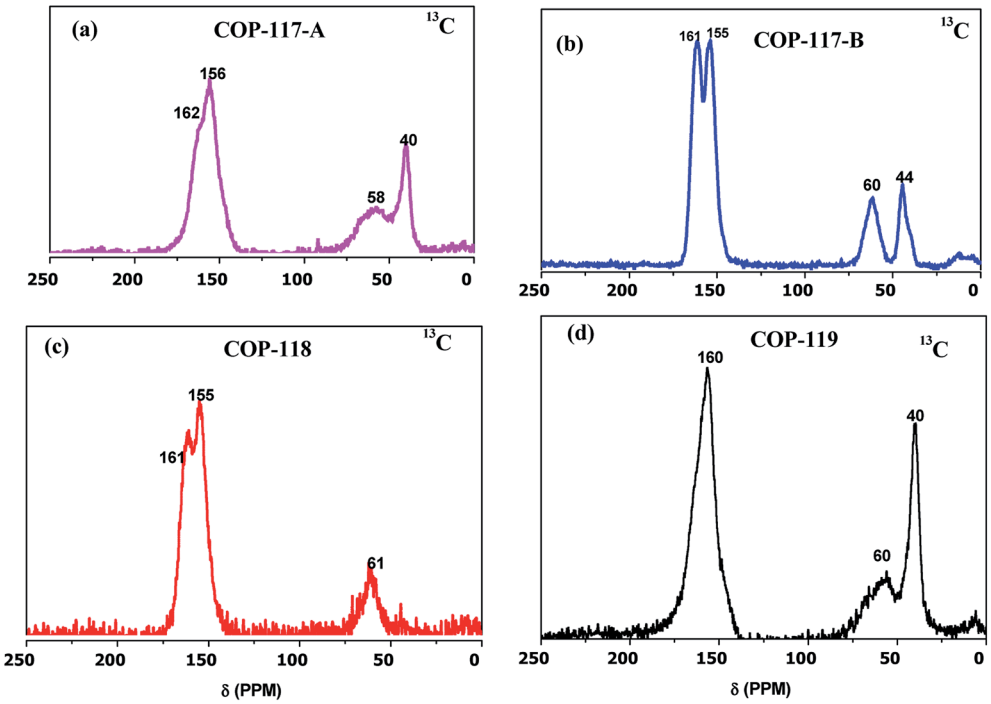

Fig. 2 Solid-state ^{13}C-NMR spectra of COPs 117-A, B, 118 and 119.

Table 1 Elemental analysis of COP materials

	% C		% H	
Materials	Experimental	Theoretical	Experimental	Theoretical
COP-117-A	81.11	91.75	6.56	8.25
COP-117-B	87.93	91.75	6.72	8.25
COP-118	72.71	84.12	4.59	7.20
COP-119	85.57	91.75	6.91	8.25

uncommon and reported in the literature for network polymers and can be attributed to external factors such as trapped moisture or solvent, or internal contamination such as leftover catalyst and unreacted methylbromides.[27,28] COP-117-A and COP-117-B have the same theoretical structure, but the measured carbon content of COP-117-A is almost 7% lower. COP-117-B has the closest experimental to theoretical values. As stated previously in NMR, the structure of COP-117-B is cleaner because of the use of zirconium chloride and possesses less crosslinking. There could also be very small amount of unreacted methylbromides in COP-117-A, the high molecular weight of bromine atoms can explain the 7% carbon difference. COP-119 has intermediate values between COP-117-A and B. COP-118 has the lowest carbon content of the reported COP structures because of the triphenylphosphine core and the theoretical 9% phosphor. The difference between experimental and theoretical values is also the highest for COP-118. This may be attributed to the different re-activities of the core used in the synthesis, triphenylphosphine being less reactive than mesitylene towards alkylation.

Table 2 represents the physical properties of all COP materials, where COP-118 has the largest surface area of 473 $m^2 g^{-1}$, and a moderate pore volume of 0.2303 cm^3/while COP-119 has the lowest surface area of 11 $m^2 g^{-1}$ and the smallest total pore volume of 0.014 $cm^3 g^{-1}$. COP-117-A has the second largest surface area with the largest total pore volume (of 0.2932 $cm^3 g^{-1}$) among all the newly prepared materials. Zhang *et al.*[29] has also reported almost similar total pore volume (0.23 $cm^3 g^{-1}$) and surface area (477 $m^2 g^{-1}$) for the conjugated micro-porous network prepared with metal catalyzed reaction techniques. COP-117-B has the greatest bulk density of 0.39 g cm^{-3} and tapped bulk density of 0.4524 g cm^{-3}, while COP-119 has the smallest bulk and tapped densities of 0.1256 and 0.1427 g cm^{-3} respectively. The larger surface area, more bulk density and lower porosity of COP-118 than COP-117-A is mainly attributable to the smaller particle size of COP-118 molecules than COP-117-A structure. The low surface area and the small total pore volume of COP-119 and COP-117-B can be attributed to the unavailability of the free voids in these amorphous structures.

It can be argued that the (i) intermolecular interaction and (ii) the interpenetration of molecules in these two compounds (COP-119 and COP-117-B) are strong enough to pack almost the entire space between the molecules and minimize the intrinsic microporosity of these amorphous compounds.[30]

Although nitrogen isotherms (Fig. 3) of these materials have clear hysteresis, which demonstrates some level of condensation and hence, porosity of the covalent organic polymers, however, the negligible adsorption at lower partial pressure *i.e.* $p/p_o < 0.1$ in case of COP-119 and COP-117-B further suggest macro porosity of these amorphous materials.[31]

Table 2 Physical properties of covalent organic polymers (COPs)

Materials	BET surface area ($m^2\ g^{-1}$)	Total pore volume ($cm^3\ g^{-1}$)	Density (g cm^{-3})		CO_2 adsorption at 1 bar (mmol g^{-1})	
			Bulk	Tapped bulk	273 K	298 K
COP-117-A	407	0.2932	0.1299	0.1476	1.72	0.99
COP-117-B	101	0.1159	0.3900	0.4524	1.0	0.56
COP-118	473	0.2303	0.1545	0.1931	1.82	1.10
COP-119	11	0.014	0.1256	0.1427	1.50	0.88

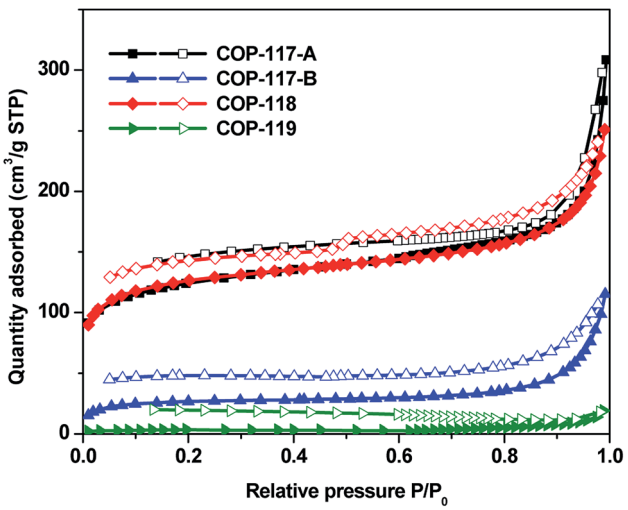

Fig. 3 Nitrogen adsorption–desorption isotherms of COP materials.

All the materials have a plateau up to the large pressure region, which corresponds to type IV characteristic as per IUPAC adsorption classification.[32] Additionally, COP-119 and COP-117-B has both the lower surface and lower total pore volume as compared to the other two compounds, where the hysteretic behavior in these two polymers is due to the distension of the polymer network.[33] As can be seen in Fig. 3, due to the very low surface area and lower total pore volume, COP-119 and COP-117-B, uptakes much lower N_2 as compared to the other two materials, suggesting less porous structure than COP-117-A and COP-118. Nitrogen isotherm loops always close at the partial pressure values of around less than the relative pressure of 0.4 indicative of microporous structures,[34] the visible hysteresis that stretch to far higher relative pressures indicate the presence of mesoporosity in these compounds. However, micropore distribution (Fig. S4 in ESI†) indicates that structures of COP-117-A and COP-118 are more microporous than the structure of COP-117-B and COP-119, where the latter has negligibly small micropore volume (about 0.003474 $cm^3\ g^{-1}$). As discussed earlier, the lower porosity of COP-117-B and COP-119 is mainly attributed to the interpenetration of the molecules within the structure; however, presence of the impurities that were not possible to remove from the final structure may also occupy the free space that subsequently reduces the porosity of these structures. Elemental analysis also suggested the existence of unreacted methylbromides in the structures that may contribute to the pore volume reduction of these two compounds.

The thermogravimetric analysis, TGA (Fig. 4) conducted in nitrogen environment indicates that all the COPs materials are highly stable and maintain their structures up to 300 °C. COP-117-A and COP-117-B which were synthesized with mesitylene as the core monomer have more robust[13] structures as compared to the other two polymers, since, a gradual and slow degradation of these two polymers observed at 350 °C. COP-117-B has shown 23% weight loss at 550 °C while COP-117-A degrades up to 58% at 800 °C. On the other hand, COP-118, which was prepared with phosphine as the core monomer has shown steep degradation up to 350 °C, however, beyond 450 °C it decompose relatively quickly than COP-117-A, B, where, almost 50% of material weight was disappeared at around 600 °C. This rapid collapse of COP-118 at the range of 450 °C and above may be either related to the flexibility of phosphine structure or to the thermal instability of the linkers molecules.[35,36] COP-119 exhibited similar performance to COP-118, but with slower decomposition rate as compared to the latter. The slow decomposition and lasting stability of COP-117-A, and B than that of COP-118, can be attributed to the stiffness of the core monomers *i.e.* mesitylene.[37]

3.2 Gas adsorption measurements

Fig. 5a and b and Table 2 represent the low pressure (up to 1 bar) and low temperature (273 K and 298 K) CO_2 uptake of all

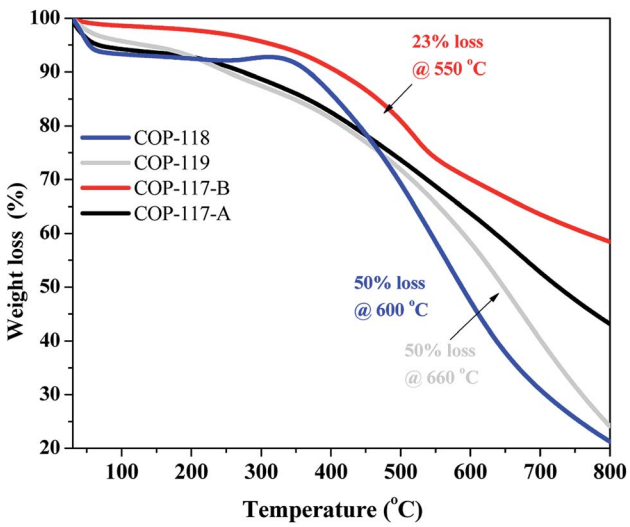

Fig. 4 Thermogravimetric analysis (TGA) of COPs materials under nitrogen atmosphere, heated up to 800 °C at the rate of 5° min^{-1}.

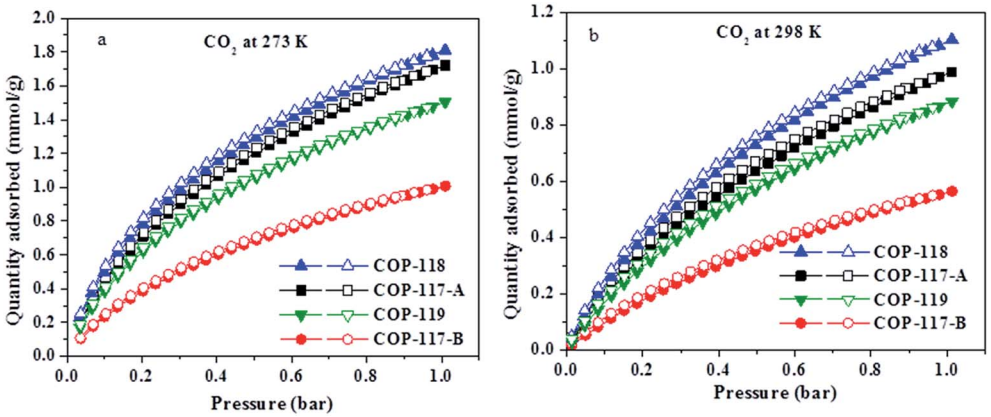

Fig. 5 CO_2 adsorption–desorption isotherms at 273 K (a) and 298 K (b) up to 1 bar.

four materials. Excluding COP-119, the CO_2 uptake (at low pressure and lower temperatures) has strong dependency on the surface areas of the materials, since the maximum adsorption capacities and the surface areas of materials have similar trends of COP-118 > COP-117-A > COP-117-B. The exceptional, lower surface area and lower pore volume but, higher up take of COP-119 than COP-118 may be the cause of the different linkers as well as different conditions used in the polymer synthesis.[37] Since the tri bromo-methyl sites in the linker of COP-119 instead of di-bromo-methyl sites, may shrink the possible pores in the structure due to the larger coordination between the adjacent core molecules. COP-118 having surface area of 473 $m^2\ g^{-1}$ (ref. 37 and 38) can adsorb up to the maximum of 1.82 mmol g^{-1} of CO_2 at 273 K which is less than 180 mg g^{-1} (4.11 mmol g^{-1}) adsorbed by hyper cross linked polymer (HCP). The lower CO_2 capturing capacity discovered in this study than the recently reported HCP by Liu *et al.*[37] can be mainly attributed to the significant differences in the pore volume and surface areas of these materials. As shown in Fig. 5, the adsorption behavior of COP-118 and COP-117-B at 273 K has almost similar trends, however slight change in the adsorption can be observed at 298 K.

The newly prepared COPs were tested for adsorption–desorption of three major gases *i.e.* CO_2, N_2 and CH_4 at two different temperatures 298 K and 323 K, and pressure up to 10 bars. Fig. 6 and Table 3 display details of the adsorption–desorption behavior of the four COPs. As can been seen in Fig. 6a and b, COP-118 has the highest CO_2 adsorption, which is followed by COP-117-A and COP-119 at room temperature and higher temperature of 323 K. Among all four COPs materials

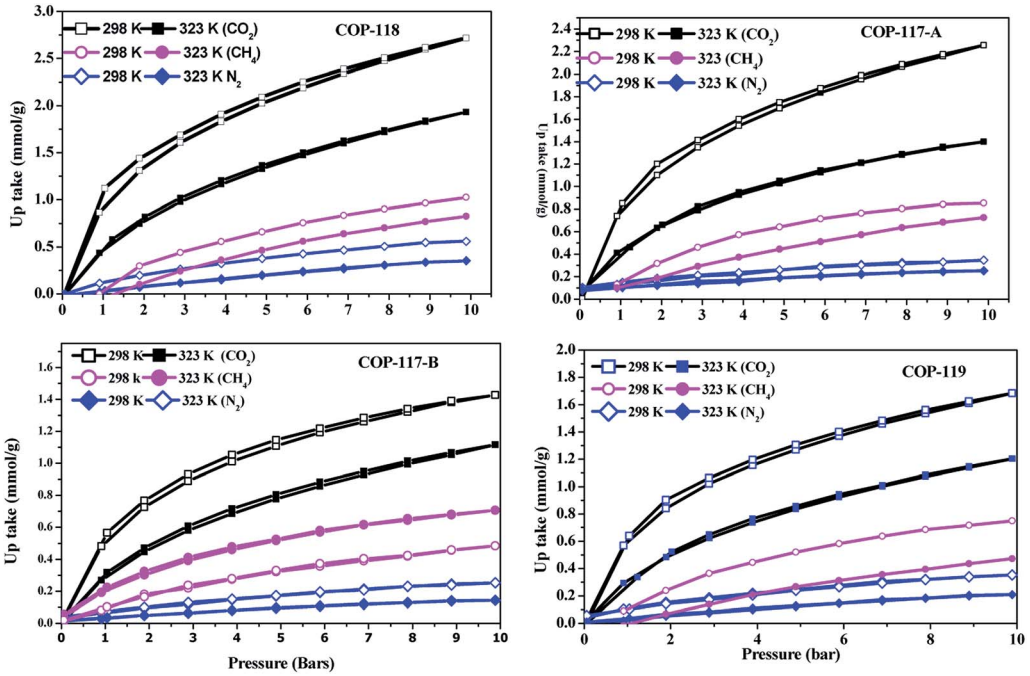

Fig. 6 CO_2, CH_4 and N_2 adsorption–desorption isotherms by COP-118, COP-117-A, COP-119 and COP-117-B at 298 K, 323 K and 10 bars.

Table 3 Maximum gas adsorption by various COPs materials at 10 bars and different temperatures

	N_2 (mmol g^{-1})		CH_4 (mmol g^{-1})		CO_2 (mmol g^{-1})		Selectivity $CO_2 : CH_4 : N_2$	
Materials	298 K	323 K	298 K	323 K	298 K	323 K	298 K	323 K
COP-117-A	0.35	0.25	0.88	0.80	2.25	1.39	6.5 : 2.5 : 1	5.5 : 3.2 : 1
COP-117-B	0.25	0.14	0.71	0.48	1.43	1.12	5.7 : 2.8 : 1	7.9 : 3.4 : 1
COP-118	0.56	0.35	1.00	0.89	2.72	1.93	4.9 : 1.8 : 1	5.5 : 2.5 : 1
COP-119	0.35	0.2083	0.78	0.50	1.69	1.20	4.8 : 2.2 : 1	5.8 : 2.4 : 1

COP-117-B has shown the least performance for CO_2 adsorption capacity both at room temperature and higher temperature up to 323 K, where the material uptake even less than 1 mmol g^{-1} of CO_2.

Fig. 6 also represents methane (Fig. 6c and d) and nitrogen (Fig. 6e and f) adsorption–desorption isotherms of all four materials at 298 K and 323 K with maximum pressure of 10 bars. It can be seen from Fig. 6c and d that, performance of COP-118 for methane up take at two different temperatures and maximum pressure of 10 bars, is better than that of other polymers. It must be noted that methane adsorption–desorption isotherms of COP-118 has almost identical trend to that of COP-117-A, except the phosphorous containing polymer has comparatively better performance as long as the maximum adsorption at 10 bars is concerned. Fig. 6c and d further reveal that at pressures lower than 2 bars COP-117-A can adsorb more methane than COP-118 at 298 K and 323 K. Importantly, both COP-119 and COP-117-B can uptake very little amount of methane at any temperature.

Fig. S5† also represents CH_4 and N_2 adsorption–desorption isotherms of all four materials at 298 K and 323 K with maximum pressure of 10 bars. The performance of COP-118 for CH_4 uptake at two different temperatures and maximum pressure of 10 bars, is better than that of other polymers. It is also noted that CH_4 adsorption–desorption isotherms of COP-118 has almost identical trend to that of COP-117-A, except the phosphorous containing polymer has comparatively better performance as long as the maximum adsorption at 10 bars is concerned. Moreover, at pressures lower than 2 bars COP-117-A seems to adsorb more CH_4 than COP-118 at 298 K and 323 K. Importantly, both COP-119 and COP-117-B can uptake very little amount of CH_4 at any temperature.

Upon comparing the adsorption behavior of all the materials for CO_2, performance of the materials varies as COP-118 > COP-117-A > COP-119 > COP-117-B, irrespective of the temperature effect. In case of CH_4 adsorption at 298 K, the uptake trends remains almost similar to that of CO_2, however, COP-117-B has lower performance than COP-119. Additionally, at 323 K the adsorption–desorption isotherms of COP-118 tends almost to be similar to that of COP-117-A, whereas COP-117-B shows same behavior as COP-119.

N_2 adsorption is comparatively much lower for all of these polymers, however, the adsorption trends varies as COP-118 > COP-117-A > COP-119 > COP-117-B both at 298 K and 323 K. Generally, among all the four different covalent organic polymers, COP-118 has shown better performance for adsorption of all the three gases at any temperature while COP-119 possess the worst performance for the adsorption of all three gases. The best performance of COP-118 for CO_2 uptake than all other covalently bonded organic polymers can be mainly attributed to its high surface area and comparatively large pore volume as compared to other three networks. A strong feature of N_2 isotherm at 77 K (Fig. 3) and CO_2 uptake isotherms at 298 K and 323 K (Fig. 5) in the terms of adsorption behavior may further suggest the effect of mesoporosity on the adsorption performance of the materials. Based on the N_2 isotherms and the pore size distribution, it was argued earlier that, structure of COP-118 and COP-117-A may be more mesoporous than that of other two polymers due to the coverage of the free space by impurity and/or intermolecular penetration in COP-117-B and COP-119.[39]

It is of most importance to understand the behavior of individual materials for three major gases namely CO_2, CH_4 and N_2, since they are the main gases to be dealt with in the energy sector as well as for the environmental protection point of view. We investigated the performance (Fig. 6) of all four materials for CO_2, CH_4 and N_2 adsorption and compared their uptakes capacities both at room temperature and a higher temperature of 323 K at the same pressure of 10 bars. All the materials almost exhibit similar performance for the three gases by capturing more CO_2 than CH_4 and N_2 respectively as shown in Fig. 6.

Another important aspect of the obtained adsorption isotherms is that, all of the four materials showed similar trends of decreasing adsorption with increasing temperature from 298 K to 323 K. It must be noted that, reduction in the adsorption of CO_2 due to the temperature effect was more pronounced for all of the materials as compared to the adsorption reduction for CH_4 and N_2. The reduction in CO_2 adsorption capacity due to temperature effect was about 39% for COP-117-A while it was measured to be 29% for COP-118 indicating performance stability of the later at higher temperature. This stable and better activity of COP-118 at higher temperature can be associated to the stiffness[40] of the pore walls and non-collapse behavior of the pores originated from the covalently bonded nature of the materials. In addition to the lowest performance as a solid adsorbent for various gases, COP-119 has also shown strong variation in adsorption capacities of gases at different temperatures, however, in case of COP-118, COP-117-A and COP-11-B temperature effect has caused very limited changes in N_2 and CH_4 adsorption.

Fig. 7 compares the maximum uptake capacity of various gases by COPs at 298 K and 323 K and maximum pressure of 10

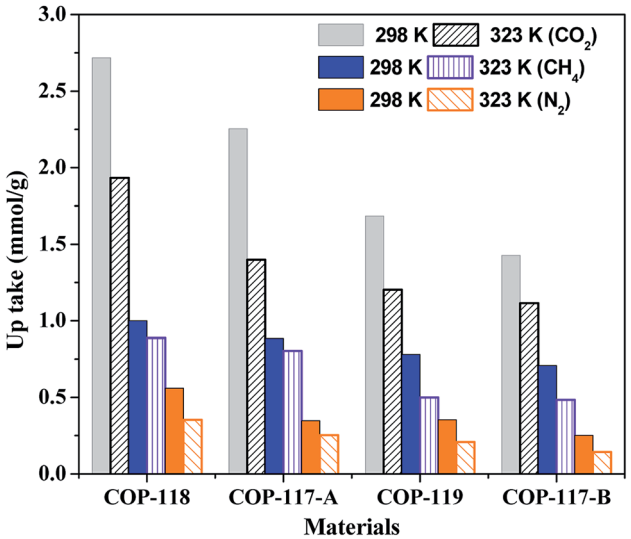

Fig. 7 Overall performance of COPs materials for the maximum adsorption of CO_2, CH_4 and N_2 at two different temperatures and maximum pressure of 10 bars.

bars. COP-118 has the highest adsorption capacity for all the gases, since it adsorbs 2.72 mmol g^{-1} of CO_2 at 298 K and 10 bars whereas COP-117-B up takes almost half of this quantity under similar condition of temperature and pressure. Although this quantity of CO_2 uptake by COP-118 is comparable to modified covalent organic polymers reported in the literature,[21] COP-118 captured much higher quantities of gases than other aromatic polymers[41,42] and COPs[13] those has higher surface areas. Table 3 displays the gas selectivity data, which is obtained based on the single gas sorption data on each polymers presented in this work.

The higher gas uptake of COP-118 can be mainly attributed both to the largest surface area and larger pore volume as compared to that of other materials *i.e.* COP-117-B and COP-119. Although, COP-117-A has larger pore volume than COP-118, however, it captures comparatively less quantity of gases than COP-118. In some cases adsorption process is often dependent on the surface area rather than the pore volume,[43] such as Patel *et al.*[12,20] have observed similar behaviour in case of unmodified and azo-group modified COP, which have higher surface area and lower pore volume but adsorbed more CO_2 than the other COPs with lower surface and larger pore volume. It is also worth mentioning here that core component of COP-118 is different than the rest of the materials, since it contains phosphorus atom coordinated with the three phenyl rings making phosphorous analogues of ammonia. Amines as functional group have high affinity for CO_2 and have been extensively used for the enhancement[40] of CO_2 adsorption on the solid sorbents.[44,45] Phosphines are strongly nucleophilic and therefore more attractive for the electropositive carbon of CO_2 in comparison to the other compounds presented herein, which subsequently enhanced the affinity and hence resulting in higher CO_2 adsorption. In addition, amine modified solid sorbents have the issue of chemisorption,[46] whereas the adsorption–desorption isotherms of CO_2 were linearly pressure depended indicating only its physical attachment to COP-118 surface and inner pores.

COP-118 has shown comparatively better performance by capturing larger quantities of various gases both at room temperature and higher temperature; however, it has low selectivity as compared to the other materials. As shown in Table 3, COP-117-A has better selectivity for $CO_2 : CH_4 : N_2$ which is 6.5 : 2.5 : 1 respectively, while this is 4.9 : 1.8 : 1 in case of COP-118 at 298 K and 10 bars. Interestingly, like azo-group modified COPs[20] with increasing temperature selectivity of COP-118 increases to higher values of 5.5 : 2.5 : 1, while, it reduces from 6.48 to 5.54 for CO_2 in the case of COP-117-A. Lower selectivity with higher CO_2 adsorption capacity and larger selectivity with lower CO_2 up take has been attributed to the nitrogen and oxygen enrichment in benzimidazole linked and benzoxazole-linked porous polymers networks at partial pressure.[47,48] As discussed earlier, COP-117-A has larger percentage reduction in the CO_2 adsorption as compared to that of COP-118 indicating the stability of the later for adsorption process at higher temperature. It can be deduced from the above discussion that, although, the selectivity of COP-117-A is larger than that of COP-118 at room temperature, but, at higher temperature (323 K), performance of the COP-117-A is weakening which would be attributed to the effect of temperature on affinity[49] and pore volume. Temperature variations brought changes both to the affinity[20] of CO_2 and also shrunk the pores within the materials due to thermal expansion of the materials.[50] We believe that, COP-118 has much higher stability in the physical parameters such as surface area, pore volume and as a result affinity of the materials remains unaffected due to temperature changes. Additionally, COP-118 can be prepared with simplified polymerization techniques and would be much economical than the rest of materials, since, the core ingredient (triphenylphosphine) of this covalently bonded polymer is relatively cheap, commercially and abundantly available and has many tunable organic properties such as non-toxicity and air stability.[51,52]

Isosteric heat of adsorption (Q_{st}) and rate of adsorption (k) for CO_2 uptake by all COPs were calculated with Clausius–Clapeyron equation[53] and linear driving force (LDF) model[54] respectively. The details of these calculations are provided in ESI document Fig. S6 and S7, Table S2 and S3.† Following Fig. 8a shows that the isosteric heat of adsorption associated with the CO_2 adsorption is increasing in case of COP-117-A and COP-117-B, while decreasing for COP-118 and COP-119 with increasing adsorbed quantity of CO_2. For the adsorbed CO_2 of 1.0 mmol g^{-1} COP-117-A and COP-118 have the adsorption heat of 35.4 kJ mol^{-1} and 29.4 kJ mol^{-1} respectively, which is reduced to 28.4 kJ mol^{-1} and 27.0 kJ mol^{-1} for COP-119 and COP-117-B. The nitrogen rich covalent organic polymers reported by Patel *et al.*[20] and microporous organic polymers[18] have almost similar heat of adsorption which is in the range of 24–32 kJ mol^{-1} as determined here for CO_2. Heat of adsorption is mainly arising from the interaction of adsorbate with the attractive sites on the surface and in the pore of adsorbent. It can be assumed that less heat will be associated with surface attachment of adsorbate due to the ease in availability of the

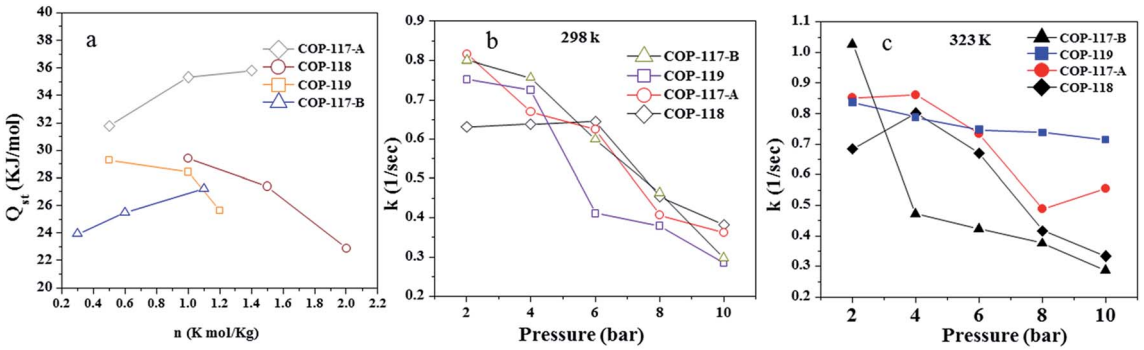

Fig. 8 (a) Heat of adsorption associated with the CO_2 adsorption; rate of CO_2 adsorption calculated; at: (b) 298 K and (c) 323 K.

attractive site instead of interaction with the inner pore attractive site. Additionally, surface heterogeneity also plays an important role in the adsorption process, because the uneven adsorbent surface would provide more attractive sites on the outer surface as compared to the interior of the pores.[55] The exterior surface of COP-118 would have large numbers of available interactions sites as compared to other materials, which will facilitate the adsorption–desorption process and would not require high-energy penalty. These significant differences in the capturing sites on the surfaces and within the pores of COP-118 may be associated to the functionalities of the building block (*i.e.* triphenylphosphine), which will have more tendency toward bonding with CO_2. The heat of adsorption is increasing in case of COP-117-A, because CO_2 mostly adsorbed within the pore of material and have high intermolecular interaction of adsorbate which subsequently liberating more heat as compared to surface adsorption.[56] In addition, surface of COP-117-A is stiffer and uniform due to the rigidity of the mesitylene structure *i.e.* building block of polymer, which further sustaining large heat of adsorption.

Fig. 8 shows the heat of adsorption and rate of adsorption data that is calculated for the COPs studied in this work. As shown in Fig. 8b and c, almost all of the materials have similar trend of lessening the rate of CO_2 adsorption with respect to pressure both at 298 K and 323 K except COP-118, which has uniform rate of adsorption initially up to 6 bars and then begins decreasing. Although, COP-118 initially captures CO_2 with slow rate up to 4 bars at 298 K, however, at higher pressures, COP-118 capture at faster rate than all other materials. Reduction in the rate of CO_2 adsorption with respect to the pressure is obvious, since, the incremental increase in the pressure is immediately after the saturation obtained at the previous pressure point. This means that, the sorbent becomes saturated at a set pressure point, where most of the pores and attractive sites become occupied by adsorbate. However, by increasing the pressure in the next step, the adsorbate takes longer time to accommodate itself within the already occupied space, which makes the adsorption rate slower with respect to the pressure.[57] As discussed earlier COP-118 may have more available sites, therefore initially, the CO_2 adsorption rate is uniform up to the pressure of 6 bars whereas in all other materials the adsorption sites are almost filled even at lower pressure. It is important to mention that adsorption rate increasing with increase in temperature while decreasing with increase in pressure for all materials. At higher temperature interaction of the adsorbent molecules with the adsorbate attractive site is energetically favourable, because CO_2 molecule is in high energy state at higher temperature and tries to attain the lower energy state by adsorbing on the attractive surface quickly, making the adsorption rate faster.

Upon introducing CO_2 to a specific COP adsorbent (COP-118), changes in the vibrational frequency in the band associated with CO_2 fundamental asymmetric stretch mode (2349 cm^{-1}) were observed, revealing changes in the CO_2 free gas situation. As shown in Fig. 9, this band was red-shifted to a wavenumber of 2334 cm^{-1} in tandem with the appearance of a lower frequency shoulder at 2322 cm^{-1}. The former change was previously encountered for CO_2 in interaction with polymers, exhibiting a red-shift (2335 cm^{-1}) that was assigned to the sorption of CO_2 in the polymer. However, no specific conclusion was made regarding whether the appearance of the lower frequency band is an indication of a unique sorption site or is a hot band. In the same plot, all reported CO_2 pressures exhibited red-shift at 2334 cm^{-1} except the bands of 0.04 and 0.1 bar which are located at a slightly higher wavenumber (2336

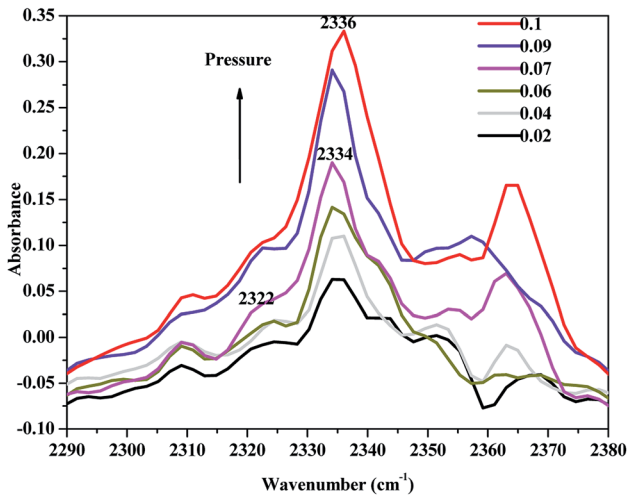

Fig. 9 *In situ* FTIR analysis of CO_2 adsorption by COP-118 at 298 K and different pressures, clearly indicating effect of pressure on adsorption process.

cm^{-1}). Moreover, an increase in the absorbance was observed to be proportional to the increase in CO_2 pressure.

4. Conclusion

In conclusion, four different covalent organic polymers have been synthesized using two different core monomers and different linkers and have been tested for capturing CO_2, CH_4 and N_2 at two different temperatures and moderate pressure of 10 bars. The surface areas and pore volumes of COP-118 and COP-117-A were found comparable to other COPs reported in the literature with the exception that COP-119 has very low surface area and small pore volume. COP-118 with the highest surface area of 473 m^2 g^{-1} and second largest volume (0.2303 cm^3 g^{-1}), among all the four materials has shown excellent performance by adsorbing 2.72 mmol g^{-1} CO_2, 1.00 mmol g^{-1} CH_4 and 0.56 mmol g^{-1} N_2 at 298 K and 10 bars. Though the surface area and pore volume influence the adsorption process, but, the nucleophilic tri-phenyl-phosphine may have contributed to the better performance of COP-118 for higher CO_2 uptake. We believe that surface of COP-118 has more alkaline nature due to the existence of phosphine in the molecular structure as compared to other COPs materials, which subsequently increases the affinity of CO_2. Like other solid sorbents CO_2 up take of COP-118 was reduced to 1.93 mmol g^{-1} at higher temperature of 323 K. Although selectivity of COP-117-A was better than that of COP-118 at room temperature, yet, the percentage reduction in CO_2 up take was lower for COP-118 than that of COP-117-A, indicating the stability in the material performance at higher temperature. Importantly, all the adsorption isotherms were exactly matching with desorption isotherms representing only the physical capture of CO_2 by COPs materials and no evidence of chemisorption was observed. Improvement in the selectivity of the materials can be achieved by further increasing the affinity of CO_2 against other gases.

Acknowledgements

This paper was made possible by the support of Qatar National Research Fund, National Priorities Research Program (NPRP) grant # 5-499-1-088. The statements made herein are solely the responsibility of the authors.

References

1 M. Ghommem, M. R. Hajj and I. K. Puri, *Ecol. Modell.*, 2012, **235–236**, 1–7.
2 C. Ekström, F. Schwendig, O. Biede, F. Franco, G. Haupt, G. de Koeijer, C. Papapavlou and P. E. Røkke, *Energy Procedia*, 2009, **1**, 4233–4240.
3 A. Giuffrida, D. Bonalumi and G. Lozza, *Appl. Energy*, 2013, **110**, 44–54.
4 P. Mores, N. Rodríguez, N. Scenna and S. Mussati, *Int. J. Greenhouse Gas Control*, 2012, **10**, 148–163.
5 C. Pritchard, A. Yang, P. Holmes and M. Wilkinson, *Process Saf. Environ. Prot.*, 2015, **94**, 188–195.
6 H. Bakhtiary-Davijany and T. Myhrvold, in *Industrial Process Scale-up*, ed. J. Harmsen, Elsevier, Amsterdam, 2013, pp. 73–98.
7 N. Hedin, L. Andersson, L. Bergström and J. Yan, *Appl. Energy*, 2013, **104**, 418–433.
8 J. Wang, L. Huang, R. Yang, Z. Zhang, J. Wu, Y. Gao, Q. Wang, D. O'Hare and Z. Zhong, *Energy Environ. Sci.*, 2014, **7**, 3478–3518.
9 J. C. Glier and E. S. Rubin, *Energy Procedia*, 2013, **37**, 65–72.
10 V. Finsy, L. Ma, L. Alaerts, D. E. De Vos, G. V. Baron and J. F. M. Denayer, *Microporous Mesoporous Mater.*, 2009, **120**, 221–227.
11 Y. Zhu, J. Zhou, J. Hu, H. Liu and Y. Hu, *Chin. J. Chem. Eng.*, 2011, **19**, 709–716.
12 H. A. Patel, F. Karadas, A. Canlier, J. Park, E. Deniz, Y. Jung, M. Atilhan and C. T. Yavuz, *J. Mater. Chem.*, 2012, **22**, 8431–8437.
13 H. A. Patel, F. Karadas, J. Byun, J. Park, E. Deniz, A. Canlier, Y. Jung, M. Atilhan and C. T. Yavuz, *Adv. Funct. Mater.*, 2013, **23**, 2270–2276.
14 H. A. Patel, M. S. Yavuz and C. T. Yavuz, *RSC Adv.*, 2014, **4**, 24320–24323.
15 H. A. Patel, S. H. Je, J. Park, Y. Jung, A. Coskun and C. T. Yavuz, *Chem.–Eur. J.*, 2014, **20**, 772–780.
16 W. Lu, D. Yuan, J. Sculley, D. Zhao, R. Krishna and H.-C. Zhou, *J. Am. Chem. Soc.*, 2011, **133**, 18126–18129.
17 Z. Xiang, X. Zhou, C. Zhou, S. Zhong, X. He, C. Qin and D. Cao, *J. Mater. Chem.*, 2012, **22**, 22663–22669.
18 R. Dawson, D. J. Adams and A. I. Cooper, *Chem. Sci.*, 2011, **2**, 1173–1177.
19 R. Dawson, E. Stockel, J. R. Holst, D. J. Adams and A. I. Cooper, *Energy Environ. Sci.*, 2011, **4**, 4239–4245.
20 H. A. Patel, S. Hyun Je, J. Park, D. P. Chen, Y. Jung, C. T. Yavuz and A. Coskun, *Nat. Commun.*, 2013, **4**, 1357.
21 J. Byun, S.-H. Je, H. A. Patel, A. Coskun and C. T. Yavuz, *J. Mater. Chem. A*, 2014, **2**, 12507–12512.
22 F. Karadas, C. T. Yavuz, S. Zulfiqar, S. Aparicio, G. D. Stucky and M. Atilhan, *Langmuir*, 2011, **27**, 10642–10647.
23 H. Yin, A. S. Sabau, J. C. Conklin, J. McFarlane and A. L. Qualls, *Appl. Energy*, 2013, **106**, 243–253.
24 M. P. Tsyurupa and V. A. Davankov, *React. Funct. Polym.*, 2002, **53**, 193–203.
25 C. D. Wood, B. Tan, A. Trewin, H. Niu, D. Bradshaw, M. J. Rosseinsky, Y. Z. Khimyak, N. L. Campbell, R. Kirk, E. Stöckel and A. I. Cooper, *Chem. Mater.*, 2007, **19**, 2034–2048.
26 G. A. Olah, S. Kobayashi and M. Tashiro, *J. Am. Chem. Soc.*, 1972, **94**, 7448–7461.
27 C. F. Martin, E. Stockel, R. Clowes, D. J. Adams, A. I. Cooper, J. J. Pis, F. Rubiera and C. Pevida, *J. Mater. Chem.*, 2011, **21**, 5475–5483.
28 Y. Yang, Q. Zhang, S. Zhang and S. Li, *RSC Adv.*, 2014, **4**, 5568–5574.
29 K. Zhang, B. Tieke, F. Vilela and P. J. Skabara, *Macromol. Rapid Commun.*, 2011, **32**, 825–830.
30 N. B. McKeown and P. M. Budd, *Macromolecules*, 2010, **43**, 5163–5176.

31 O. Okay, *Prog. Polym. Sci.*, 2000, **25**, 711–779.
32 X. Zhuang, F. Zhang, D. Wu and X. Feng, *Adv. Mater.*, 2014, **26**, 3081–3086.
33 B. G. Hauser, O. K. Farha, J. Exley and J. T. Hupp, *Chem. Mater.*, 2012, **25**, 12–16.
34 M. Kruk and M. Jaroniec, *Chem. Mater.*, 1999, **12**, 222–230.
35 Q. Zhang, Y. Yang and S. Zhang, *Chem.–Eur. J.*, 2013, **19**, 10024–10029.
36 T. Ni, F. Xing, M. Shao, Y. Zhao, S. Zhu and M. Li, *Cryst. Growth Des.*, 2011, **11**, 2999–3012.
37 G. Liu, Y. Wang, C. Shen, Z. Ju and D. Yuan, *J. Mater. Chem. A*, 2015, **3**, 3051–3058.
38 B. Li, Z. Guan, X. Yang, W. D. Wang, W. Wang, I. Hussain, K. Song, B. Tan and T. Li, *J. Mater. Chem. A*, 2014, **2**, 11930–11939.
39 R. Haldar, N. Sikdar and T. K. Maji, *Mater. Today*, 2015, **18**, 97–116.
40 C. R. Mason, L. Maynard-Atem, K. W. J. Heard, B. Satilmis, P. M. Budd, K. Friess, M. Lanč, P. Bernardo, G. Clarizia and J. C. Jansen, *Macromolecules*, 2014, **47**, 1021–1029.
41 T. Ben, H. Ren, S. Ma, D. Cao, J. Lan, X. Jing, W. Wang, J. Xu, F. Deng, J. M. Simmons, S. Qiu and G. Zhu, *Angew. Chem.*, 2009, **121**, 9621–9624.
42 Y. Yuan, F. Sun, L. Li, P. Cui and G. Zhu, *Nat. Commun.*, 2014, **5**, 4260–4267.
43 W. Wang and D. Yuan, *Sci. Rep.*, 2014, **4**, 5711–5718.
44 M. L. Pinto, L. Mafra, J. M. Guil, J. Pires and J. Rocha, *Chem. Mater.*, 2011, **23**, 1387–1395.
45 V. Zelenak, D. Halamova, L. Gaberova, E. Bloch and P. Llewellyn, *Microporous Mesoporous Mater.*, 2008, **116**, 358–364.
46 X. Yan, S. Komarneni and Z. Yan, *J. Colloid Interface Sci.*, 2013, **390**, 217–224.
47 M. G. Rabbani and H. M. El-Kaderi, *Chem. Mater.*, 2012, **24**, 1511–1517.
48 H. A. Patel, D. Ko and C. T. Yavuz, *Chem. Mater.*, 2014, **26**(23), 6729–6733.
49 K.-Y. A. Lin and A.-H. A. Park, *Energy Environ. Sci.*, 2011, **45**, 6633–6639.
50 R. Orwoll, in *Physical Properties of Polymers Handbook*, ed. J. Mark, Springer, New York, 2007, pp. 93–101.
51 L. Bai, L. Zhang, Y. Liu, X. Pan, Z. Cheng and X. Zhu, *Polym. Chem.*, 2013, **4**, 3069–3076.
52 A. B. Charette, A. A. Boezio and M. K. Janes, *Org. Lett.*, 2000, **2**, 3777–3779.
53 W. Lu, D. Yuan, D. Zhao, C. I. Schilling, O. Plietzsch, T. Muller, S. Bräse, J. Guenther, J. Blümel, R. Krishna, Z. Li and H.-C. Zhou, *Chem. Mater.*, 2010, **22**, 5964–5972.
54 A. Awadallah-F and S. Al-Muhtaseb, *Adsorption*, 2013, **19**, 967–977.
55 S. A. Al-Muhtaseb and J. A. Ritter, *J. Phys. Chem. B*, 1999, **103**, 2467–2479.
56 M. Murialdo, N. P. Stadie, C. C. Ahn and B. Fultz, *J. Phys. Chem. C*, 2015, **119**, 944–950.
57 N. A. Rashidi, S. Yusup and B. H. Hameed, *Energy*, 2013, **61**, 440–446.